

# Characterization of H5N1 Influenza Virus Variants with Hemagglutinin Mutations Isolated from Patients

Yohei Watanabe,<sup>a,b</sup> Yasuha Arai,<sup>a</sup> Tomo Daidoji,<sup>b</sup> Norihito Kawashita,<sup>c,d</sup> Madiha S. Ibrahim,<sup>e</sup> Emad El-Din M. El-Gendy,<sup>e</sup> Hiroaki Hiramatsu,<sup>f</sup> Ritsuko Kubota-Koketsu,<sup>g</sup> Tatsuya Takagi,<sup>c,d</sup> Takeomi Murata,<sup>h</sup> Kazuo Takahashi,<sup>i</sup> Yoshinobu Okuno,<sup>g</sup> Takaaki Nakaya,<sup>b</sup> Yasuo Suzuki,<sup>f</sup> Kazuyoshi Ikuta<sup>a</sup>

Department of Virology, Research Institute for Microbial Diseases, Osaka University, Osaka, Japan<sup>a</sup>; Department of Infectious Diseases, Graduate School of Medical Science, Kyoto Prefectural University of Medicine, Kyoto, Japan<sup>b</sup>; Graduate School of Pharmaceutical Sciences, Osaka University, Osaka, Japan<sup>c</sup>; Genome Information Research Center, Research Institute for Microbial Diseases, Osaka University, Osaka, Japan<sup>d</sup>; Department of Microbiology and Immunology, Faculty of Veterinary Medicine, Damanhour University, Damanhour, Egypt<sup>e</sup>; Health Scientific Hills, College of Life and Health Sciences, Chubu University, Aichi, Japan<sup>f</sup>; Kanonji Institute, The Research Foundation for Microbial Diseases of Osaka University, Kagawa, Japan<sup>g</sup>; Department of Applied Biological Chemistry, Faculty of Agriculture, Shizuoka University, Shizuoka, Japan<sup>h</sup>; Department of Infectious Diseases, Osaka Prefectural Institute of Public Health, Osaka, Japan<sup>i</sup>

Y.W. and Y. A. contributed equally to this work.

**ABSTRACT** A change in viral hemagglutinin (HA) receptor binding specificity from  $\alpha 2,3$ - to  $\alpha 2,6$ -linked sialic acid is necessary for highly pathogenic avian influenza (AI) virus subtype H5N1 to become pandemic. However, details of the human-adaptive change in the H5N1 virus remain unknown. Our database search of H5N1 clade 2.2.1 viruses circulating in Egypt identified multiple HA mutations that had been selected in infected patients. Using reverse genetics, we found that increases in both human receptor specificity and the HA pH threshold for membrane fusion were necessary to facilitate replication of the virus variants in human airway epithelia. Furthermore, variants with enhanced replication in human cells had decreased HA stability, apparently to compensate for the changes in viral receptor specificity and membrane fusion activity. Our findings showed that H5N1 viruses could rapidly adapt to growth in the human airway microenvironment by altering their HA properties in infected patients and provided new insights into the human-adaptive mechanisms of AI viruses.

**IMPORTANCE** Circulation between bird and human hosts may allow H5N1 viruses to acquire amino acid changes that increase fitness for human infections. However, human-adaptive changes in H5N1 viruses have not been adequately investigated. In this study, we found that multiple HA mutations were actually selected in H5N1-infected patients and that H5N1 variants with some of these HA mutations had increased human-type receptor specificity and increased HA membrane fusion activity, both of which are advantageous for viral replication in human airway epithelia. Furthermore, HA mutants selected during viral replication in patients were likely to have less HA stability, apparently as a compensatory mechanism. These results begin to clarify the picture of the H5N1 human-adaptive mechanism.

Received 15 January 2015 Accepted 27 February 2015 Published 7 April 2015

**Citation** Watanabe Y, Arai Y, Daidoji T, Kawashita N, Ibrahim MS, El-Gendy EE-DM, Hiramatsu H, Kubota-Koketsu R, Takagi T, Murata T, Takahashi K, Okuno Y, Nakaya T, Suzuki Y, Ikuta K. 2015. Characterization of H5N1 influenza virus variants with hemagglutinin mutations isolated from patients. *mBio* 6(2):e00081-15. doi:10.1128/mBio.00081-15.

**Editor** Terence S. Dermody, Vanderbilt University School of Medicine

**Copyright** © 2015 Watanabe et al. This is an open-access article distributed under the terms of the [Creative Commons Attribution-NonCommercial-ShareAlike 3.0 Unported license](https://creativecommons.org/licenses/by-nc-sa/4.0/), which permits unrestricted noncommercial use, distribution, and reproduction in any medium, provided the original author and source are credited.

Address correspondence to Yohei Watanabe, nabe@biken.osaka-u.ac.jp.

Although human infections by avian influenza (AI) viruses of subtypes H7N9, H6N1, H10N8, and H9N2 (1, 2) have recently drawn attention, the pandemic potential of highly pathogenic avian influenza virus (HPAIV) subtype H5N1 remains alarming and is of increasing concern because of the virus's complex ecology and diversification in the field (3, 4).

Hemagglutinin (HA), the most abundant surface antigen of the influenza virion, is a trimeric protein (5). The HA monomer has a globular head region and a stalk region and has two main functions. The first HA function is viral attachment to host cells, which is mediated by specific binding between the receptor binding domain (RBD) of the HA head region and the cell receptor (6). Influenza viruses recognize terminal sialic acid (Sia) and galactose linkage patterns on sialylglycans. Human influenza viruses pref-

erentially bind to  $\alpha 2,6$ -linked Sia ( $\alpha 2,6$  Sia) that is expressed on human upper airway epithelia, whereas most avian viruses preferentially bind to a sugar chain ending in  $\alpha 2,3$ -linked Sia ( $\alpha 2,3$  Sia) that is expressed on bird intestinal epithelia. This presents an interspecies barrier that prevents AI viruses from easily infecting humans. The second HA function is membrane fusion after viral endocytosis, which is mediated by the fusion domain in the HA stalk region (7). Membrane fusion is triggered by low endosomal pH, which induces irreversible conformational changes in HA, leading to insertion of the HA fusion domain into the endosomal membrane, fusion of the viral and endosomal membranes, and release of the viral genome into the cell. Different HA subtypes have a range of pH and temperature stability phenotypes and, therefore, have different fusion characteristics and inactivation kinetics (8, 9).

H5N1 HPAIV has become endemic in birds in some areas, including China, Vietnam, and Egypt. Continuous circulation has allowed the H5N1 virus to diverge genetically to form phylogenetically and phenotypically distinct clades (designated clades 0 to 9) in different geographic areas. In particular, clade 2.2.1, which is unique to Egypt, has the most striking features. Clade 2.2.1 viruses have acquired many human-adaptive mutations that can facilitate AI virus replication and transmission in mammals (10, 11). Egypt is now regarded as a hot spot for H5N1 virus evolution with increased bird-to-human transmission efficacy (12). Therefore, investigation of the human-adaptive mutations that clade 2.2.1 viruses might acquire in patients should provide valuable data for risk assessment and control strategies against an H5N1 pandemic. However, the human-adaptive changes in H5N1 viruses, including clade 2.2.1 viruses from patients, have not been fully investigated. To address this, we conducted a comprehensive analysis of the effects on the viral phenotype of the HA mutations that have been selected in clade 2.2.1 viruses isolated from Egyptian patients. These results provide the first broad-spectrum data on HA characteristics that have been selected in H5N1 viruses in infected patients and new insight into H5N1 evolution in humans.

## RESULTS

### Identification of human-adaptive mutations in clade 2.2.1 HAs.

We searched for HA genes with amino acid mutations that presumably had been selected by viral replication in H5N1-infected patients via a database search of HA sequences in human and bird H5N1 viruses isolated in Egypt during 2006 to 2010. This yielded 94 human virus HA sequences and 343 bird virus HA sequences from the National Center for Biotechnology Information Influenza Virus Resource (NCBI IVR). At the time of this investigation, the 94 human virus and 343 bird virus HA sequences represented 100% and 76%, respectively, of the complete and partial H5N1 virus sequences from Egypt in the NCBI IVR. All the sequences were from viruses isolated from clinical swabs or samples that had been passaged no more than three times in eggs and/or cultured cells (see Table S1 in the supplemental material). Since preliminary experiments showed that virus variants with *in vitro* adaptive mutations that were selected during virus propagation in eggs/cells did not become dominant in the viral population until after more than six passages (data not shown), the HA sequences in this study should represent the original viral population in the infected hosts.

A consensus HA sequence for the H5N1 viruses in Egypt was determined by aligning all the Egyptian H5N1 virus HA sequence data. HA mutations in the 94 human and 343 bird H5N1 virus strains were identified by comparing the HA sequences in these strains to the consensus sequence. Based on their prevalences in the human and bird viruses, the mutations were classified in two categories: mutations that were only in human virus strains and mutations with a higher prevalence in human virus strains than in bird virus strains (Table 1). Of the 21 mutations in the HA globular head region, 10 were found only in human virus strains and 11 had a higher prevalence in human virus strains than in bird virus strains. Of these 21 mutations, the N94D (change of N to D at position 94) mutation was located at the interface of the trimeric HA, and the remaining 20 mutations were located on the HA surface around the RBD. The five mutations in the HA stalk region were found only in human virus strains. These results were in agreement with the human-adaptive mutations found using a

TABLE 1 Prevalences in human and bird viruses of H5N1 HA mutations identified in a database search

HA region	Category of mutation	Mutation in HA (H5 numbering)	% of strains with mutation (no. of strains) <sup>a</sup> among:	
			Human viruses	Bird viruses
Head	Only in human viruses	H125Y	4.3 (4)	0 (0)
		V131M	1.1 (1)	0 (0)
		A134S	1.1 (1)	0 (0)
		A134V	1.1 (1)	0 (0)
		K152Q	2.1 (2)	0 (0)
		N182K	1.1 (1)	0 (0)
		A184G	2.1 (2)	0 (0)
		T195I	1.1 (1)	0 (0)
		S223N	4.3 (4)	0 (0)
		S223I	1.1 (1)	0 (0)
	More prevalent in human viruses than in bird viruses	N94D	15.9 (15)	3.4 (12)
		A127T	2.1 (2)	0.9 (3)
		I28Δ	52.1 (49)	22.2 (76)
		I151T	52.1 (49)	22.2 (76)
		D154N	30.9 (29)	30.3 (104)
		D154E	1.1 (1)	0.3 (1)
		D154G	2.1 (2)	1.4 (5)
		T188I	3.2 (3)	2.3 (8)
		R189G	1.1 (1)	0.3 (1)
		R189S	1.1 (1)	0.9 (3)
		Q192H	4.3 (4)	2.0 (7)
More prevalent in bird viruses than in human viruses (control)	A184E	4.3 (4)	32 (110)	
	A185E	3.2 (3)	12 (42)	
	A185T	3.2 (3)	3.2 (11)	
		L190I	1.1 (1)	24.1 (83)
Stalk	Only in human viruses	Q15H	2.1 (2)	0 (0)
		K22R	1.1 (1)	0 (0)
		K28R	2.1 (2)	0 (0)
		K35R	1.1 (1)	0 (0)
		K48E	1.1 (1)	0 (0)

<sup>a</sup> There were 94 human virus strains and 343 bird strains in this study.

novel phylogenetic algorithm (13), confirming the identification of these mutations in the database search in this study. We also identified four RBD mutations that were more prevalent in bird virus strains than in human virus strains and included them in further studies as controls.

There were 18 multiple mutations that were only found in human viruses, five multiple mutations with a higher prevalence in human viruses than in bird viruses, and four multiple mutations with a higher prevalence in bird viruses than in human viruses that were included in these studies as controls (see Table S2 in the supplemental material). To identify the residue(s) in these multiple mutations responsible for viral human adaptation, we also studied HAs with single and small (e.g., double) mutations that were part of these larger mutations (Table S3). For example, an H5N1 virus with the HA H125Y/D154N/N94D triple mutation was isolated from a patient, but the H125Y single mutation and H125Y/N94D double mutation were not detected in any virus from patients in this study. Therefore, we generated and studied

H5N1 HAs with the H125Y, H125Y/N94D, and H125Y/D154N/N94D mutations.

In all, 59 single and multiple mutations were investigated in this study (see Tables S2 and S3 in the supplemental material) to determine the effects of H5 HA mutations on the viral phenotype, using reverse genetics in the genetic background of A/duck/Egypt/D1Br/2007 (EG/D1), which is one of the parental H5N1 clade 2.2.1 strains. Among these mutations, we previously reported that the Q192H and 128 $\Delta$ /I151T mutations increased the binding affinity of HA for  $\alpha$ 2,6 Sia (14).

#### Sia binding specificities of H5N1 viruses with HA mutations.

The acquisition of binding affinity for long  $\alpha$ 2,6 sialylglycans has been reported to be important for AI virus adaptation to humans (15). Therefore, we carried out direct binding assays using sialylglycopolymers of different lengths to determine the effects of HA mutations on viral  $\alpha$ 2,3 Sia and  $\alpha$ 2,6 Sia binding affinities. Glycans with one, two, or three lactosamine (LN) repeats were used for the  $\alpha$ 2,3 sialylglycopolymers ( $\alpha$ 2,3 SLN1,  $\alpha$ 2,3 SLN2, and  $\alpha$ 2,3 SLN3, respectively) and  $\alpha$ 2,6 sialylglycopolymers ( $\alpha$ 2,6 SLN1,  $\alpha$ 2,6 SLN2, and  $\alpha$ 2,6 SLN3, respectively). The glycans with SLN2 and SLN3 were considered long sialylglycans. For this study, several virus strains were used as control or reference viruses: A/Suita/64/2011 (Suita/64), A/Suita/113/2011 (Suita/113), and A/Suita/114/2011 (Suita/114), which are seasonal human H3N2 strains; A/Japan/434/2003 (Japan/434; H3N2) and A/Puerto Rico/8/34 (PR8; H1N1), which are laboratory human strains; and A/Duck/Hong Kong/820/80 (Duck/HK/820; H5N3), which is a classical AI virus strain.

The results of virus binding assays using  $\alpha$ 2,3 SLN1,  $\alpha$ 2,6 SLN1, and  $\alpha$ 2,6 SLN2 are shown in Fig. S1 in the supplemental material. All the human influenza viruses used as controls had binding affinities for  $\alpha$ 2,6 Sia. In particular, clinical H3N2 strains Suita/64, Suita/113, and Suita/114 had strong binding to  $\alpha$ 2,6 SLN2. However, laboratory strains Japan/434 (H3N2) and PR8 (H1N1) had higher affinities than the clinical strains for both  $\alpha$ 2,3 SLN1 and  $\alpha$ 2,6 SLN1. In contrast, the classical AI virus Duck/HK/820 (H5N3) and EG/D1 (wild type [wt]) had strong binding affinity only for  $\alpha$ 2,3 SLN1. Most of the H5N1 human virus variants with an HA head mutation(s) had increased binding affinity for  $\alpha$ 2,6 Sia. Some of the mutations (i.e., H125Y, N182K, S223N, and N94D) resulted in an appreciable decrease in  $\alpha$ 2,3 Sia binding and an increase in  $\alpha$ 2,6 Sia binding.

The apparent association constant ( $K_a$ ) was determined by nonlinear regression curve fitting, and receptor binding specificity was expressed as the  $K_a$  for each sialylglycopolymer divided by that for  $\alpha$ 2,3 SLN1 (14, 16). The results (Fig. 1A and B) indicated that most mutations in the HA head region of human viruses increased virus binding specificity for both  $\alpha$ 2,6 SLN1 and  $\alpha$ 2,6 SLN2 an average of 14- and 20-fold, respectively, relative to the binding specificities of EG/D1 (wt) virus for these sialylglycopolymers. However, mutations in the HA head region of bird viruses produced minimal increases in binding specificity for  $\alpha$ 2,6 Sia, and none of the mutations in the HA stalk region had a significant effect on  $\alpha$ 2,6 Sia binding specificity. Increased binding specificity for  $\alpha$ 2,6 SLN3, the longest  $\alpha$ 2,6 sialylglycan in this study, was only observed in mutants with a few specific mutations that were only found in human virus HAs (Fig. 1C).

However, the  $\alpha$ 2,6 Sia binding specificities of the virus variants were lower than those of human influenza viruses, particularly the seasonal influenza virus Suita strains (Fig. 1D to F). The binding specificity differences between H5N1 human and bird viruses

were greater for longer  $\alpha$ 2,6 sialylglycopolymers, i.e., the difference was least for  $\alpha$ 2,6 SLN1, greater for  $\alpha$ 2,6 SLN2, and greatest for  $\alpha$ 2,6 SLN3. In contrast, the binding specificity for long  $\alpha$ 2,3 sialylglycopolymers was relatively constant among the H5N1 viruses. The average binding specificities of the virus variants for  $\alpha$ 2,3 SLN2 and  $\alpha$ 2,3 SLN3 were 1.41- and 0.99-fold, respectively, of those of EG/D1 (wt) virus (see Fig. S2 in the supplemental material). These results indicated that most RBD mutations selected by viral growth in patients increased the binding specificity of H5N1 virus for long  $\alpha$ 2,6 sialylglycans.

**Replication of H5N1 viruses in human airway epithelial cell cultures.** To investigate the effect(s) of H5 mutations on viral replication in human cells, primary human small airway epithelial (SAE) cells were infected with H5N1 viruses and seasonal human viruses at a multiplicity of infection (MOI) of 0.1, and progeny viral RNA production and viral cytopathogenicity were monitored for 72 h postinfection.

In SAE cells, the growth of virus variants with HA mutations that increased the binding specificity for  $\alpha$ 2,6 Sia was generally higher than that of EG/D1 (wt) at 24 h postinfection (Fig. 2A). However, the growth of the mutants was different at 48 and 72 h postinfection (Fig. 2B and C). The H125Y, H125Y/N94D, A134V/128 $\Delta$ /I151T, N182K, N182K/T195I, N182K/T195I/N94D, S223N, and S223N(I)/128 $\Delta$ /I151T HA mutants produced, on average, 7.7- and 9.7-fold more progeny virus RNA than did EG/D1 (wt) virus at 48 and 72 h postinfection, respectively. In contrast, the V131M/128 $\Delta$ /I151T, A134S/128 $\Delta$ /I151T, R140K/128 $\Delta$ /I151T, K152Q/128 $\Delta$ /I151T, K152Q/D154N/128 $\Delta$ /I151T, A184G/128 $\Delta$ /I151T, and A184G/D154N/128 $\Delta$ /I151T/Q15H HA mutants produced, on average, 4.0-fold more progeny virus RNA than did EG/D1 (wt) virus at 48 h postinfection and an amount similar to that produced by EG/D1 (wt) virus (an average of 1.6-fold more progeny virus RNA) at 72 h postinfection. However, H5N1 produced significantly less progeny virus RNA (i.e., had significantly slower growth) than seasonal human viruses (Fig. 2D to F), e.g., H5N1 EG/D1 (wt) produced approximately 100-fold less progeny virus RNA than human viruses at 24 h postinfection (Fig. 2A and D). However, mutants with increased progeny virus RNA production at 24 and 48 h postinfection produced progeny viral RNA at levels comparable to those of human viruses at 72 h postinfection (Fig. 2C and F).

Infection of SAE cells with the HA mutant viruses produced progeny virus titers that were several log greater than for infection with EG/D1 (wt) (Fig. 3A), consistent with the effect of HA mutations on progeny virus RNA production. Although the HA mutations in this study produced less than 15-fold more progeny virus RNA than EG/D1 (wt), the progeny virus titers of the HA mutant viruses were several log (up to 10<sup>3</sup>-fold) greater than that of EG/D1 (wt). These results confirmed that the HA mutations in this study had significant effects on H5N1 replication. The increases in the growth kinetics of the mutant viruses correlated with their increased cytopathogenicity in SAE cells (Fig. 3B).

These results suggested that the H5N1 mutations selected during viral infection of humans increased clade 2.2.1 virus replication in human airway epithelia. Interestingly, mutations that increased  $\alpha$ 2,6 Sia specificity did not always increase viral replication in human airway epithelial cells. Some mutant viruses with comparable levels of  $\alpha$ 2,6 Sia specificity showed an increase in replication, and some showed a decrease in replication. These results indicated that the binding specificity of HA for human-type re-

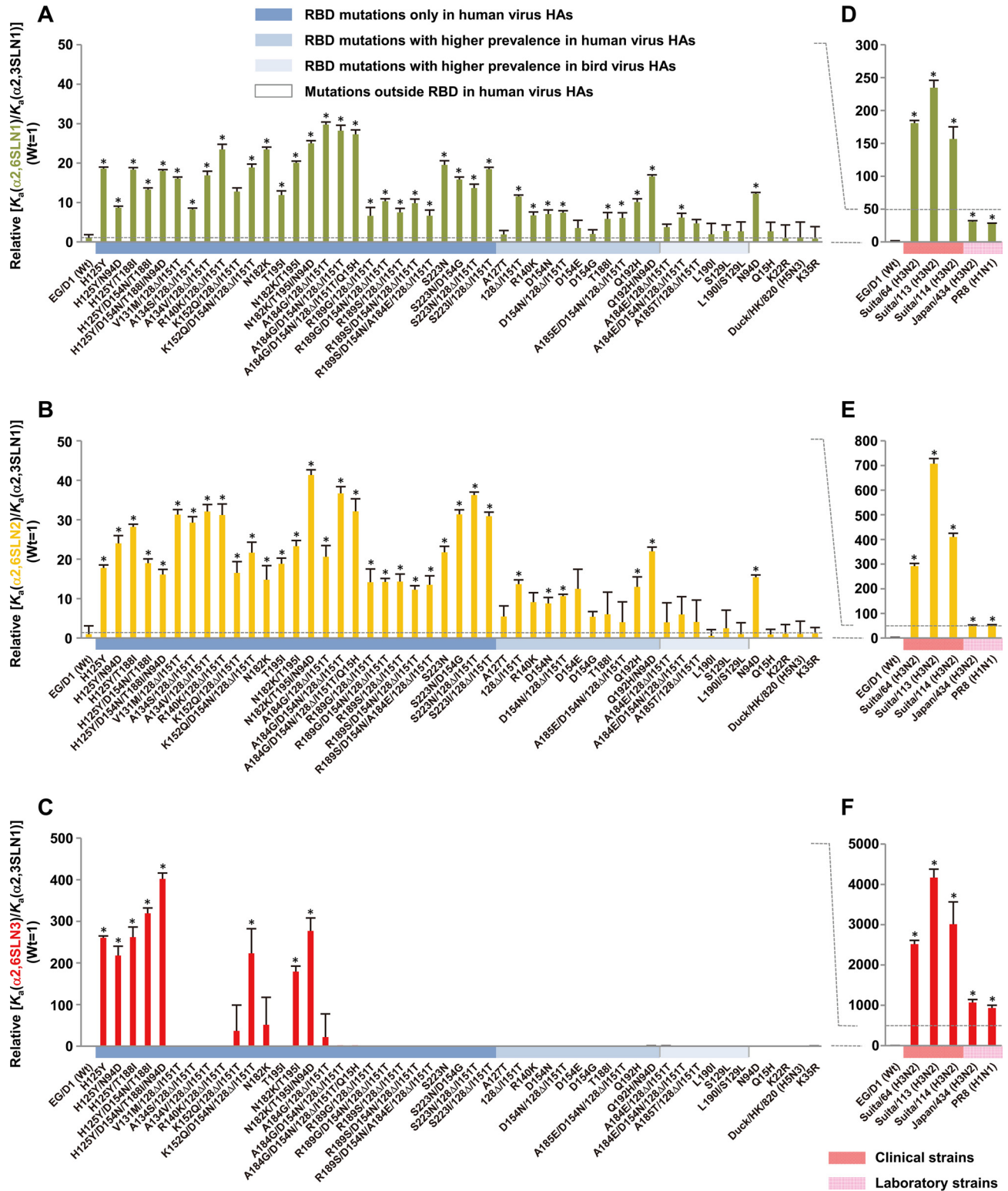


**FIG 1** Effects of HA mutations on receptor binding specificities relative to the results for EG/D1 (wt) virus HA. Apparent association constants ( $K_a$ ) were determined by nonlinear regression fitting of receptor binding data (see Fig. S1 in the supplemental material). The receptor binding specificities for  $\alpha 2,6$  SLN1 (A and D),  $\alpha 2,6$  SLN2 (B and E), and  $\alpha 2,6$  SLN3 (C and F) are expressed as  $K_a(\alpha 2,6 \text{ SLN1})/K_a(\alpha 2,3 \text{ SLN1})$ ,  $K_a(\alpha 2,6 \text{ SLN2})/K_a(\alpha 2,3 \text{ SLN1})$ , and  $K_a(\alpha 2,6 \text{ SLN3})/K_a(\alpha 2,3 \text{ SLN1})$ , respectively. The data are expressed relative to the results for EG/D1. Each data point is the mean  $\pm$  standard deviation (SD) from three independent experiments. The specificities of EG/D1 HA variants (A, B, and C) are compared with those of seasonal human viruses (D, E, and F). As a control, the data for a classical H5N3 strain, Duck/HK/820, are also shown. Colors on the x axis highlight the categories of HA mutations (A, B, and C) and virus strains (D, E, and F) as indicated. \*,  $P < 0.01$  (Student's  $t$  test).

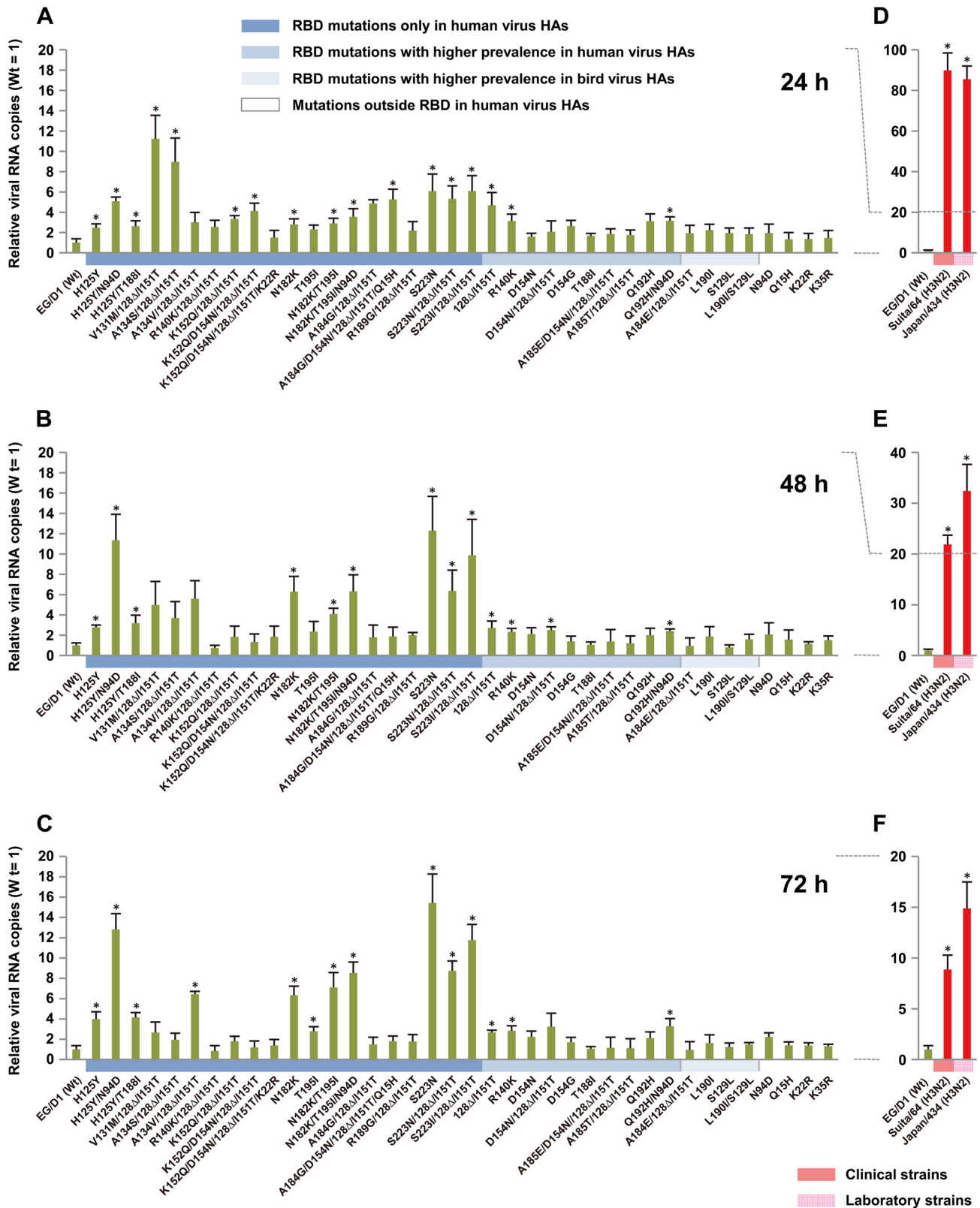


**FIG 2** Effects of HA mutations on viral replication in primary human airway cells. Small airway epithelial cells were infected with viruses at an MOI of 0.1. The culture supernatants were harvested at 24 (A and D), 48 (B and E), and 72 (C and F) h postinfection and assayed by quantitative real-time RT-PCR to determine the amount of progeny virus RNA. The amounts of progeny virus RNA produced by the HA mutant viruses (A, B, and C) and the seasonal human viruses (D, E, and F) are expressed relative to the amount produced by EG/D1 (wt) virus. Each data point is the mean  $\pm$  SD from triplicate experiments. Colors on the x axis highlight the categories of HA mutations (A, B, and C) and virus strains (D, E, and F) as indicated. \*,  $P < 0.01$  (Student's *t* test).

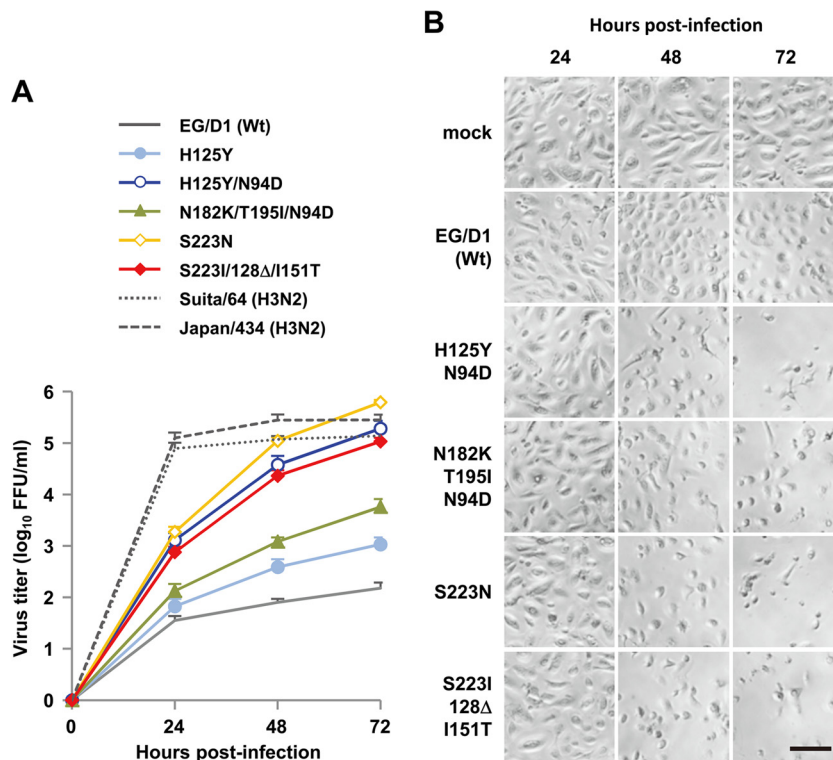


**FIG 3** Growth kinetics of EG/D1 (wt) and HA mutant viruses in primary human airway cells. Small airway epithelial (SAE) cells were infected with the indicated viruses at an MOI of 0.1. (A) The culture supernatants were harvested at the indicated times and assayed for FFU to determine progeny infectious virus titers. Each data point is the mean  $\pm$  SD from triplicate experiments. (B) Phase contrast microscopy of morphological changes in SAE cells infected by the indicated viruses at an MOI of 0.1 and examined at the indicated times postinfection. Scale bar represents 250  $\mu$ m.

ceptors was not the sole determinant of H5N1 growth kinetics in human airway epithelia, prompting us to investigate other factors that affect H5N1 replication in the human airway. Therefore, we investigated the membrane fusion function of HA.

**pH threshold of HA activation for membrane fusion.** To assess the effect of HA mutations on low-pH-induced HA membrane fusion activity, we examined the pHs at which the membrane fusion activity of EG/D1 (wt) HA and variant virus HAs was activated. The membrane fusion activity of EG/D1 (wt), A/Shanghai/1/2006 (Shanghai/1; clade 2.3.4), and A/crow/Kyoto/53/04 (Kyoto/53; clade 2.5) H5 HAs was induced when the pH was reduced to 5.6 (Fig. 4A and C), indicating that these HAs had a typical H5N1 pH threshold for membrane fusion. Interestingly, all the mutations that increased both  $\alpha$ 2,6 Sia binding specificity and progeny virus production also raised the pH threshold for membrane fusion to  $\geq$ 5.7, i.e., to pH 5.7 for H125Y, H125Y/T188I, and H125Y/D154N/T188I mutants, pH 5.8 for A134V/128 $\Delta$ /I151T, S223N, and S223N(I)/128 $\Delta$ /I151T mutants, and pH 5.9 for N182K and N182K/T195I mutants. The results also showed that these mutant HAs were less stable at higher pHs than EG/D1 (wt) HA (see Fig. S3 in the supplemental material). However, HAs with mutations that increased  $\alpha$ 2,6 Sia binding specificity and decreased progeny virus production had pH thresholds similar to the wild-type pH threshold for membrane fusion, e.g., pH 5.6 for the V131M/128 $\Delta$ /I151T mutant. An exceptional reduction of the pH threshold for membrane fusion to 5.5 was observed for strains with the L190I mutation, which was more prevalent in bird viruses than in human viruses.

**HA expression and cleavage.** To investigate the effects of mutations on the expression and cleavage of the HA protein, 293T cells were transfected with HA expression plasmids. At 24 h post-transfection, HA proteins from cell lysates were analyzed by Western blotting. Quantitative analysis showed that HA mutants with higher pH thresholds for membrane fusion (e.g., the H125Y and S223N mutants) had lower HA expression (Fig. 5). However, there was no significant difference in the level of HA cleavage among the HA mutants. These results indicated that the increased pH threshold for membrane fusion of the variants in this study was due to qualitative changes in HA as opposed to quantitative changes, such as increased variant HA expression.

These results led us to question whether the HA variants with efficient replication in the human airway were transmissible viruses. Recent reports noted that HA stability is one of the determinants for airborne transmission of influenza viruses (17, 18). Therefore, we studied the effects of HA mutations on HA stability.

**Thermostability of H5N1 variants.** The thermostability of HA has been used as a surrogate measure of HA stability (19–21). Therefore, samples containing 128 hemagglutinating units (HAU) of EG/D1 and the HA mutants were incubated at 50°C or 54°C, and hemagglutination inactivation was measured at a number of time points. The HAU titers were plotted as a function of time (see Fig. S4 in the supplemental material), and the time required to reduce the titer of each virus to 8 HAU was calculated (Fig. 6A and B). EG/D1 (wt) and contemporary Egyptian strains A/chicken/Egypt/C1Tr13/2007 (EG/CT) and A/chicken/Egypt/RIMD12-3/

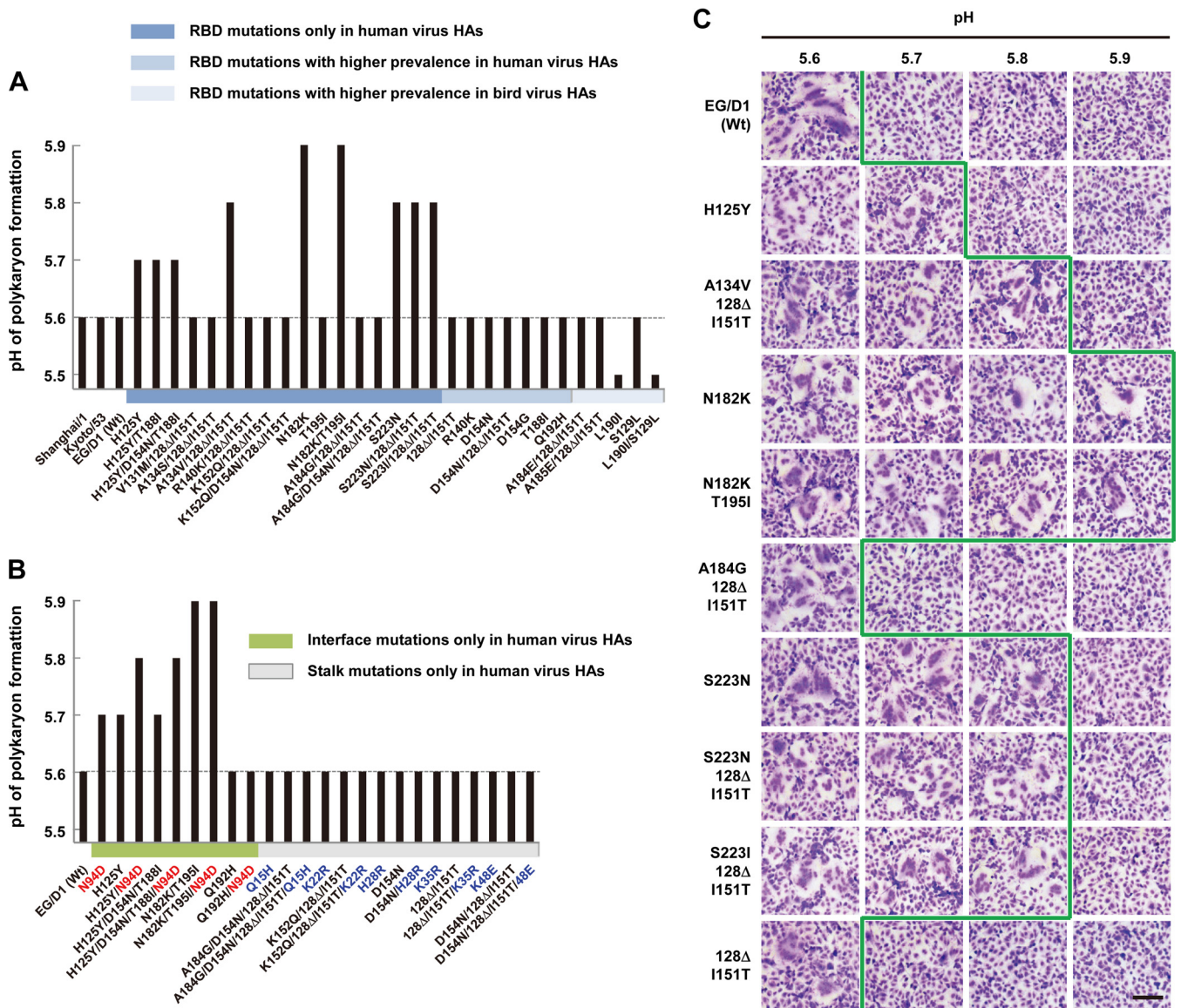


**FIG 4** pH threshold of HAs for membrane fusion activity. CV-1 cells were transfected with expression plasmids carrying EG/D1 (wt) or a mutant HA. At 24 h posttransfection, cell–cell fusion was induced by treatment with fusion buffer with a pH of 5.2 to 6.0 and the pH threshold, the highest pH value at which HA induced polykaryon formation, was monitored. (A) Effects of mutations at the surface of the HA1 trimer on the pH threshold. (B) Effects of mutations at the interface and stalk region of the HA trimer. Mutations at the interface and stalk are shown in red and blue, respectively. Some data from panel A are included for comparison. Colors on the x axis highlight the categories of HA mutations as indicated. (C) Representative fields of cells expressing the indicated HAs and exposed to pH 5.6 to 5.9. Scale bar represents 250  $\mu$ m. The green line marks the border of pH values for HA membrane fusion activity.

2008 (EG/12) had similar inactivation kinetics, indicating that the thermostability of EG/D1 (wt) was consistent with the thermostability of clade 2.2.1 viruses. Interestingly, almost all of the HA mutants with increased progeny virus production (i.e., the H125Y, H125Y/T188I, H125Y/D154N/T188I, A134V/128 $\Delta$ /I151T, N182K, N182K/T195I, S223N, and S223I/128 $\Delta$ /I151T mutants) were less thermostable than EG/D1 (wt). These results indicated that HA mutant viruses with increased progeny virus production in human epithelia were less thermostable than EG/D1 (wt).

#### Effects of mutations outside the RBD on HA properties.

Studies to generate ferret-transmissible H5N1 viruses reported that mutations at the HA interface and stalk regions enabled these viruses to be efficiently transmitted via respiratory droplets (17,

18). Therefore, we evaluated the effects of mutations at the interface and stalk regions on the properties of the HA mutants in this study. The N94D mutation at the HA interface increased both HA  $\alpha$ 2,6 Sia specificity and the pH threshold for membrane fusion and decreased HA thermostability (Fig. 1, 4B, and 6C and D). In addition, the two substitutions in the H125Y/N94D double mutant acted cooperatively in both increasing the pH threshold for membrane fusion and decreasing HA thermostability. The N182K/T195I/N94D and Q192H/N94D mutations also reduced HA thermostability in an additive manner. However, mutations in the stalk region had minimal effects on these HA properties. None of these mutations acted cooperatively to increase HA stability. These results indicated that the mutations in the HA inter-

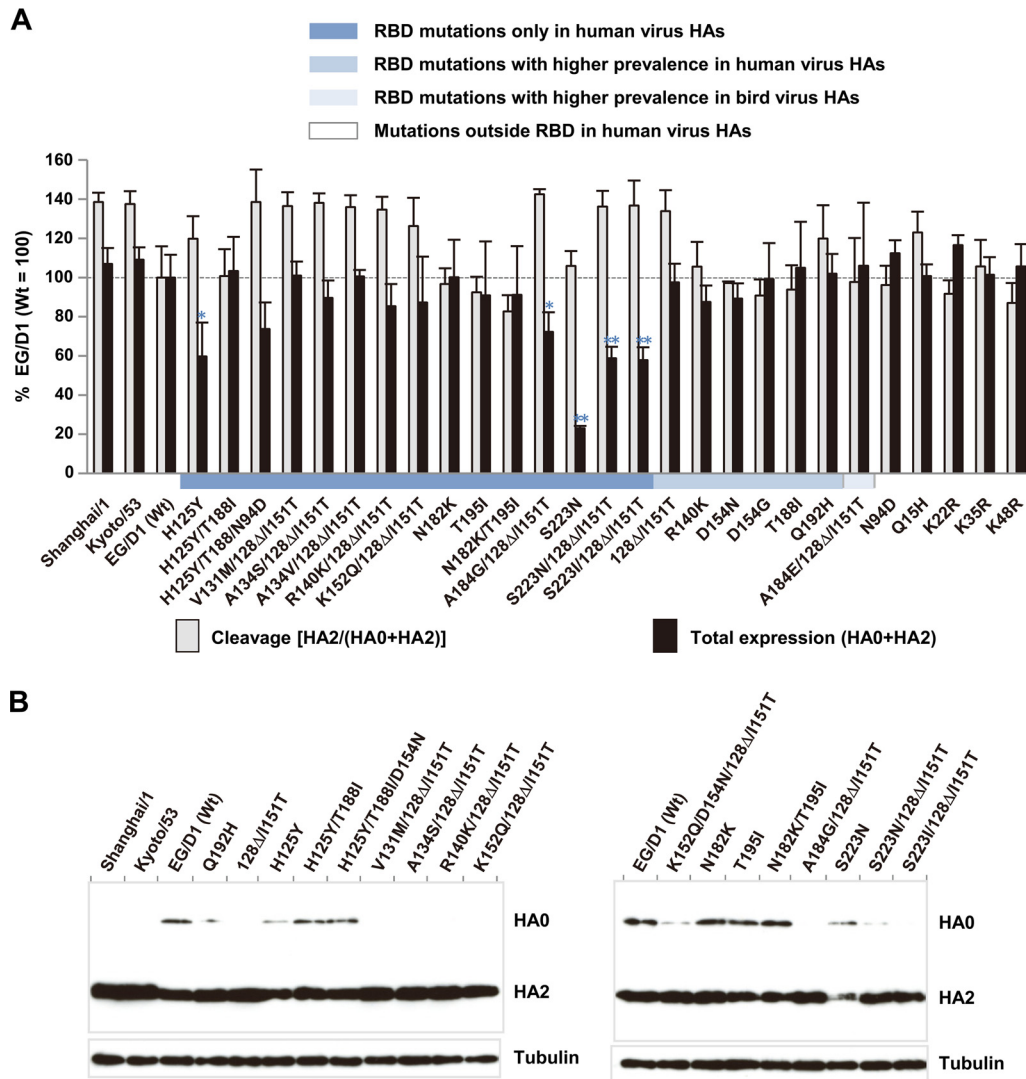


**FIG 5** Expression and cleavage of wild-type and mutant HA proteins in 293T cells. 293T cells were transfected with Flag-tagged HA expression plasmids. At 24 h posttransfection, cells were harvested and analyzed by Western blotting using anti-Flag antibody. (A) After quantitation of the band intensities by using ImageJ software, the amounts of expression and cleavage for each HA were calculated relative to those for EG/D1 (wt). Each data point is the mean  $\pm$  SD from three independent experiments. Colors on the x axis highlight the categories of HA mutations as indicated. \*\*,  $P < 0.01$ ; \*,  $P < 0.05$  (Student's *t* test). (B) Representative results of Western blotting for EG/D1 and the indicated HA mutants are shown.

face regions in this study, selected by viral replication in humans, decreased HA thermostability.

**Properties of HA that promoted viral replication in the human airway.** We next investigated the relationship between HA properties and viral replication in human airway cells. Scatter plots showed that, among the multiple HA mutations that increased  $\alpha 2,6$  Sia specificity, some of the mutations that increased the pH threshold for membrane fusion also increased viral replication in human airway cells (Fig. 7A and B, green circles). In addition, an increase in the pH threshold for membrane fusion was strongly correlated with a decrease in HA thermostability ( $R = -0.77$ ) and an increase in viral replication in human cells ( $R = 0.79$ ) (Fig. 7C and D). Taken together, these results suggested that, among virus variants selected during human infection, variants with increases in both  $\alpha 2,6$  Sia specificity and pH threshold for membrane fusion also had increased replication in human airway epithelia.

**Effect of mutations on viral replication in mice *in vivo*.** To assess the relevance of the *in vitro* results of this study to *in vivo* infections, BALB/c mice were inoculated intranasally with different dilutions of selected virus mutants. Mice infected with EG/D1 (wt) showed no clinical effects during the 14-day observation period. In contrast, mice inoculated with  $3 \times 10^4$  focus-forming units (FFU) of any of the mutants showed considerable weight loss (Fig. 8A). In addition, several mice infected with  $3 \times 10^3$  FFU of the H125Y/N94D, S223N, or S223I/128 $\Delta$ /I151T mutant died. The mutants were substantially more lethal than wild-type virus: the 50% mouse lethal doses (MLD<sub>50</sub>) were  $1.2 \times 10^4$  FFU for the H125Y and N182K/T195I/N94D mutants,  $4.4 \times 10^3$  FFU for the H125Y/N94D mutant,  $2.0 \times 10^3$  FFU for the S223N mutant, and  $7.1 \times 10^3$  FFU for the S223I/128 $\Delta$ /I151T mutant (see Fig. S5 in the supplemental material), as much as 60 times less than the MLD<sub>50</sub> of  $1.2 \times 10^5$  FFU for EG/D1 (wt). Consistent with this result, the viral yield in lungs of mice infected with  $3 \times 10^4$  FFU of



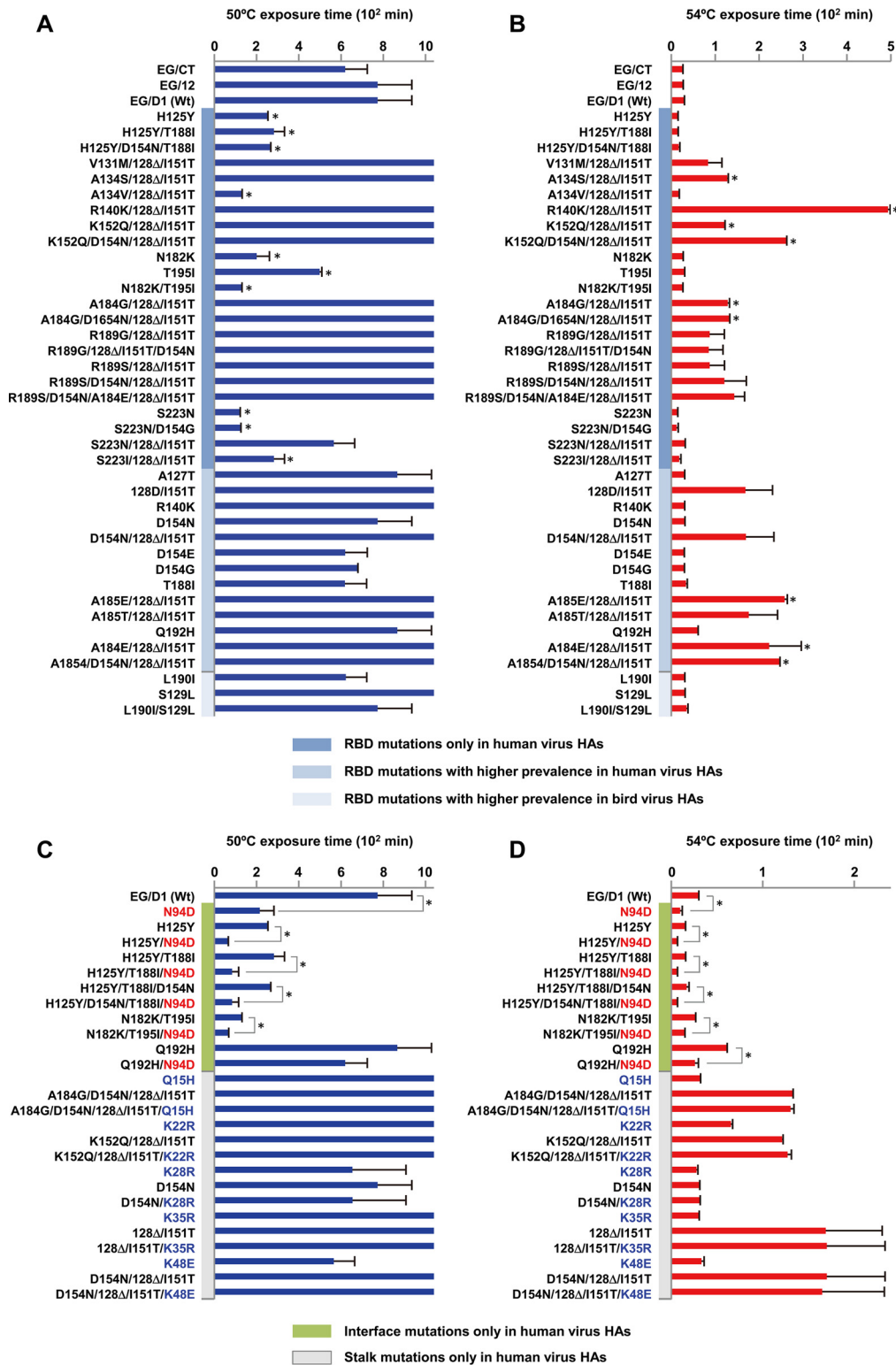


**FIG 6** Effects of HA mutations on HA thermostability. A sample containing 128 HAU of each virus was incubated at 50°C (A and C) or 54°C (B and D). Hemagglutination titers of the heat-treated samples were determined as a function of time by hemagglutination assays. The time required for the hemagglutination activity of each virus to decrease to 8 HAU was calculated by fitting the thermostability data with the Boltzmann equation (see Fig. S4 in the supplemental material). (A and B) Effects on thermostability of mutations on the surface of HA1 trimers. (C and D) Effects on thermostability of mutations at the interface and stalk region of HA trimers. Mutations at the interface and stalk are shown in red and blue, respectively. Each data point is the mean  $\pm$  SD from three experiments, which were each performed in triplicate. Colors on the y axis highlight the categories of HA mutations as indicated. Some data in the upper panels (A and B) are included in the lower panels (C and D) for comparison. \*,  $P < 0.01$  (Student's  $t$  test).

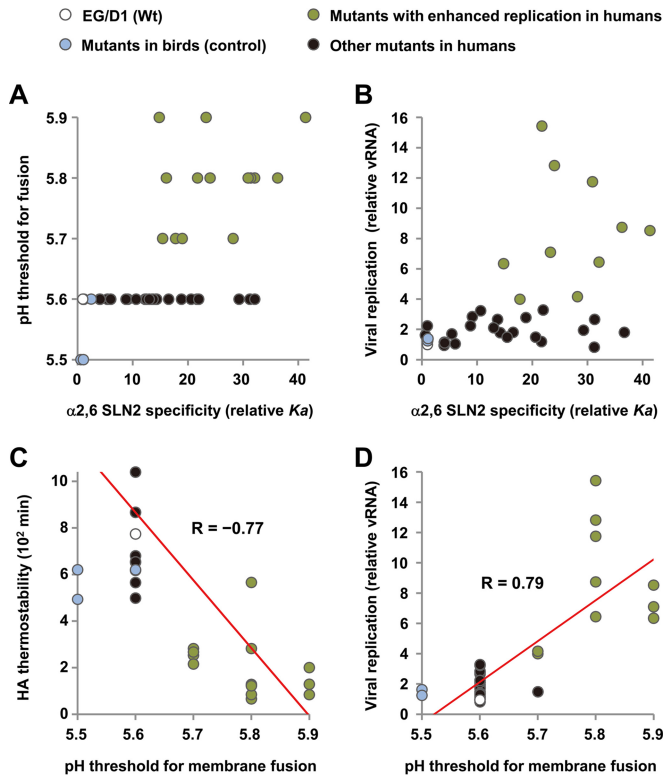


**FIG 7** Analyses of HA and viral replication in primary human airway cells. (A and B) Scatter plots of HA  $\alpha 2,6$  SLN2 specificity (x axis) versus pH threshold for HA membrane fusion activity (A) and viral replication (B) (y axis).  $\alpha 2,6$  SLN2 specificity and viral replication are calculated as  $K_a(\alpha 2,6$  SLN2)/ $K_a(\alpha 2,3$  SLN1) and progeny viral RNA (vRNA) copies, respectively, relative to the results for EG/D1 (wt). (C and D) Scatter plots of the pH threshold (x axis) versus HA thermostability (C) and viral replication (D) (y axis) with a linear fit of the data. The HA thermostability measure is the time required for viral hemagglutination activity to decrease from 128 to 8 HAU at 50°C.

the variants was >10-fold higher at 3 days postinfection and >720-fold higher at 6 days postinfection than with EG/D1 (wt) (Fig. 8C). These results indicated that mutations that enhanced viral replication in human airway epithelial cells also increased viral replication in mice *in vivo*.

**Effect of mutations on structural changes in EG/D1 HA.** To investigate the structural basis for the changes in the functional properties of HA in mutant viruses, we generated a structural model of EG/D1 HA. In this model, most of the mutations that increased  $\alpha 2,6$  Sia specificity clustered around the RBD, implying a direct role for these mutations in modifying the interaction between the host cell sialylglycan receptor and the viral RBD (see Fig. S6A and B in the supplemental material). The N94D mutation, which was located at the 110 helix structure in the vestigial esterase subdomain of the RBD and at the interface of trimeric HA, was an exception. N94D enabled the formation of an internal hydrogen bond between the Asp amino group at residue 94 and the Glu carboxy group at residue 227 (Fig. S6C). The distance between N94 of one HA monomer and T204 of another monomer, which was the closest residue to N94, was 6.20 Å, and the distance between D94 and T204 was 4.35 Å. The shorter distance with the N94D mutation should permit the formation of a repulsive electronic interaction between the oxygen atoms of the two residues. Therefore, the N94D mutation may affect the contact

between two HA monomers, modifying the thermostability of HA trimers and the HA pH threshold for membrane fusion activity.

## DISCUSSION

Repeated bird-to-human transmission may generate H5N1 variants that have greater fitness for human infections than wild-type H5N1 viruses (22). In a study of ferret-transmissible H5N1 viruses, a small number of HA mutations enabled the viruses to be efficiently transmitted via airborne droplets (21, 23). These results suggested that human-transmissible H5N1 viruses could emerge by acquiring HA mutations, although these viruses would also require other adaptations for human infections, e.g., in polymerase genes, such as PB2-627K (24). However, thus far, information on HA mutations that might be selected in humans has been limited (25). In this study, we investigated human adaptation of HA variants that were selected in H5N1-infected patients and characterized the variants that replicated more efficiently in primary human airway cultures and in mouse lungs. To our knowledge, this is the first report to systematically evaluate the effects of HA mutations selected in H5N1-infected patients on AI virus adaptation to infect humans. However, we also wish to emphasize that, in this study, we characterized HA mutations that enabled H5N1 viruses to adapt to replication in the human airway microenvironment but not HA mutations that enhanced viral airborne transmission in humans, because influenza virus airborne transmission in mammals is thought to be largely due to viral growth in the upper respiratory tract, not in the lungs.

Fitness for binding long  $\alpha 2,6$  sialylglycans has been reported to be crucial for the adaptation and pandemic spread of AI viruses in humans (15). Mutations that only increased the binding specificity for long  $\alpha 2,6$  sialylglycans were not found in this study. Almost all of the virus variants with mutations found in this study had increased binding specificity for both short and long  $\alpha 2,6$  sialylglycans (Fig. 1). This was consistent with the location of these mutations, adjacent to the RBD (see Fig. S6 in the supplemental material). Human airway epithelial cells express substantial amounts of both short and long  $\alpha 2,6$  sialylglycans (26). Therefore, H5N1 viruses may acquire HA mutations that enable binding to both types of sialylglycans to effectively increase their binding affinity for human airway epithelia. Indeed, in this study, mutant H5N1 viruses with binding specificity for both  $\alpha 2,6$  SLN1 and  $\alpha 2,6$  SLN2 replicated efficiently in human airway epithelial cells (Fig. 2 and 3). Moreover, the clinical H3N2 strains in this study also had binding affinity for both short and long  $\alpha 2,6$  sialylglycans (Fig. 1).

Cell type-dependent endosomal pH is important for influenza virus infection (27, 28). Therefore, mutations during host adaptation may enable influenza viruses to optimize the pH threshold of their HA membrane fusion activity. In this study, some HA mutations in viruses isolated from patients had an increased pH threshold for membrane fusion, from 5.6 up to 5.9 (Fig. 4). Interestingly, viruses with an increased HA pH threshold also had increased human-type receptor specificity (Fig. 7A, green circles). This concurrence between increased HA  $\alpha 2,6$  Sia binding specificity and increased HA pH threshold for membrane fusion was also observed during host adaptation in the ferret transmission studies (18, 21), with the pH thresholds shifting from 5.6 to 5.8. Recent reports suggested that differences in HA membrane fusion activity among AI virus subtypes might influence their infectivity (29, 30). These results suggested that low endosomal pH levels in human respiratory epithelia may limit infections even by HPAIV

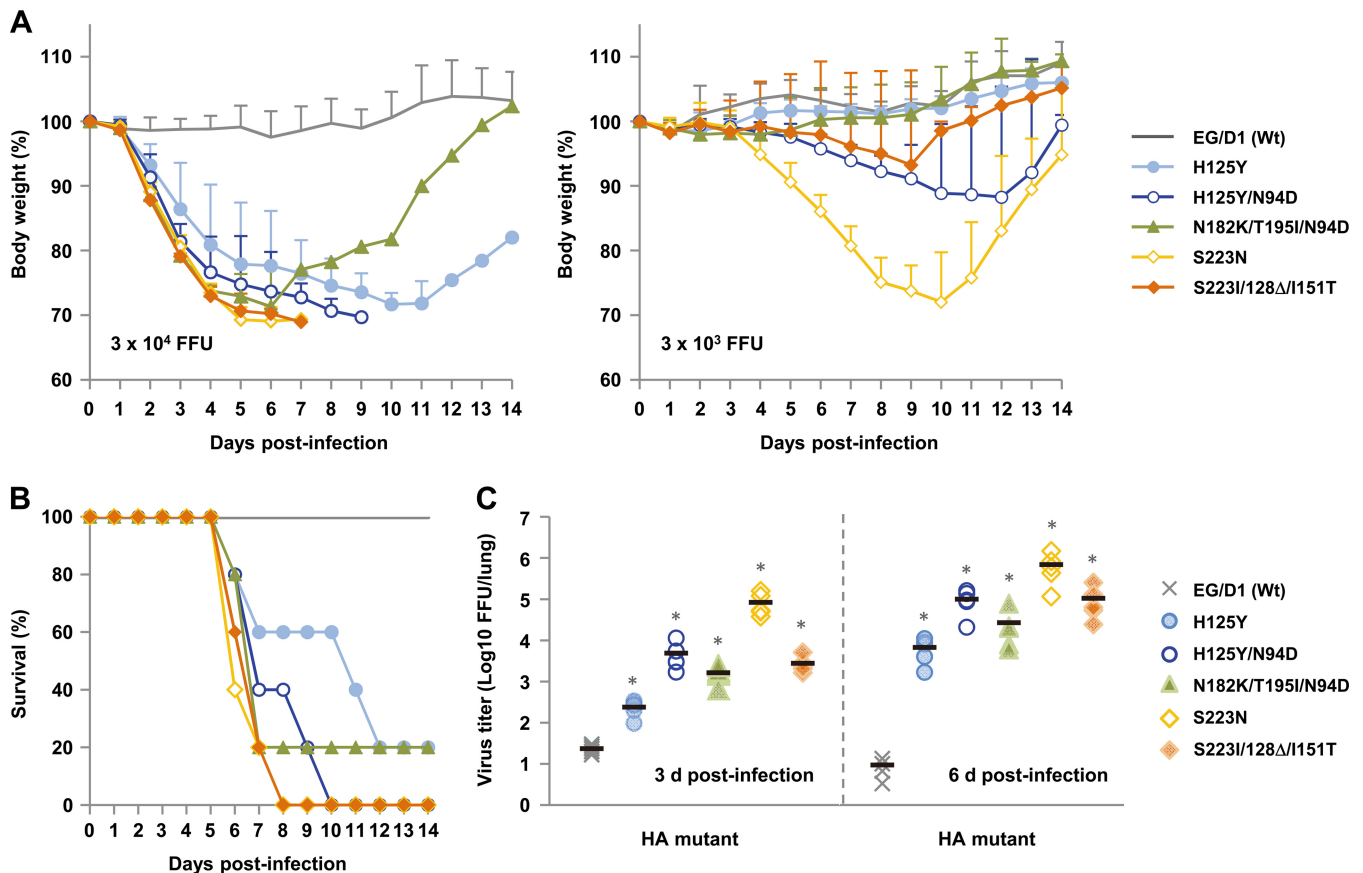


**FIG 8** Effects of HA mutations on mortality and weight loss of mice. Five-week-old BALB/c mice (5 mice per group) were inoculated intranasally with serial 10-fold dilutions of the indicated viruses. (A) Body weight of mice infected with  $3 \times 10^4$  FFU (left) or  $3 \times 10^3$  FFU (right) viruses was monitored for 14 days postinfection. The mean percent body weight change  $\pm$  SD for each group of mice is shown. (B) Survival of mice infected with  $3 \times 10^4$  FFU viruses. Calculation of mortality includes mice that were sacrificed because they had lost more than 30% of their body weight. (C) Virus titers in lungs of mice infected with  $3 \times 10^4$  FFU viruses at 3 days (left) and 6 days (right) postinfection. Each symbol indicates the value for an individual mouse. \*,  $P < 0.01$ .

H5N1 viruses that have HA pH thresholds for membrane fusion that are generally higher than those of classical AI viruses (9). To more effectively increase replication in human respiratory epithelia, H5N1 variants may acquire HA mutations that produce an increase in both  $\alpha$ 2,6 Sia binding specificity and the HA pH threshold for optimal membrane fusion. However, too much of an increase in the HA pH threshold may result in greater loss of viral infectivity, because the human upper airway mucosa pH is slightly acidic (31). Interestingly, similar changes in HA properties have been identified during human seasonal influenza virus adaptation to infect mice, in which HA mutations change the Sia binding specificity and elevate the optimal HA pH fusion threshold to increase both virulence and replication in the mouse lung (32–34). These results imply analogous HA functional changes during influenza virus adaptation to different hosts.

In this study, HA mutants with decreased thermostability also had increased pH thresholds for membrane fusion (from pH 5.6 up to 5.9) (Fig. 7C). This result was in agreement with previous reports showing an inverse correlation between the influenza virus HA pH threshold for membrane fusion and its thermostability (19, 20). The decrease in HA expression in the HA mutants in this study (Fig. 5) was probably related to the decrease in HA thermo-

stability. Therefore, most HA mutants with efficient replication in human cells had both increased  $\alpha$ 2,6 Sia binding specificity and decreased thermostability. Decreased HA stability should not be advantageous for the persistence of viral infectivity in the field, which may explain the observation that HA mutations conferring decreased thermostability have not been detected in viruses from birds (Table 1). In contrast, mutations that increased both  $\alpha$ 2,6 Sia binding specificity and HA thermostability were not frequently detected in viruses from patients. In addition, these mutations (e.g., R140K/128 $\Delta$ /I151T and K152Q/D154N/128 $\Delta$ /I151T) did not contribute to efficient viral replication in human airway cells (Fig. 2). A previous study reported that the A/Vietnam/1203/2004 (clade 1) variant with increased HA stability (the pH threshold for fusion decreased from 5.6 to 5.3) had reduced replication activity in primary human bronchial epithelial cells, and a similar result was observed in Vero, MDCK, and A549 cells, although the results were not as conclusive in these cell lines (35). Several studies showed slight differences in the growth of variants with altered HA pH thresholds for fusion in cultured cells or animals (28, 35–37). This difference may be due to the genetic background of the viruses, each with an HA with a distinct pH threshold for fusion, and the analytical conditions used.

Taken together, our findings suggested that there was selective

pressure on H5N1 viruses in infected human respiratory epithelia, primarily to increase viral  $\alpha$ 2,6 Sia binding specificity and sometimes to change both the HA pH threshold for membrane fusion and the HA thermostability. Moreover, variants with both an increase in  $\alpha$ 2,6 Sia binding specificity and an increase in the HA pH threshold for membrane fusion to pH 5.8 to 5.9 replicated more efficiently in human airway cells. However, HA mutants selected during viral replication in patients are likely to lose HA stability, apparently to compensate for the increases in  $\alpha$ 2,6 Sia binding specificity and in the pH threshold for membrane fusion, both of which are advantageous for viral replication in human airway epithelia.

Some mutations that increase the  $\alpha$ 2,6 Sia binding specificity of EG/D1 HA have been reported to also increase the human-type receptor preferences of other H5N1 clades (21, 38–41). However, this study is the first report on the effect of the N94D mutation on HA properties. In two studies of ferret-transmissible H5N1 viruses (17, 18, 21, 42), both T318I, adjacent to the HA fusion domain, and H110Y, at the HA interface region, were independently selected and stabilized HA, enabling efficient transmission of the viruses between ferrets. Although the N94D mutation is located close to HA residue 110 (see Fig. S6 in the supplemental material), it reduced HA stability. Therefore, the effect of the N94D mutation on HA stability in this study was opposite that of the T318I and H110Y mutations in the ferret study. In the structural model generated in this study, the N94D mutation permitted the formation of both an internal hydrogen bond with E227 within the same monomer and a repulsive electronic interaction with T204 in a different monomer in trimeric HA. This suggested that N94D both strengthened the interaction within one HA monomer and weakened the interaction between two different monomers in trimeric HA, thereby destabilizing trimeric HA.

Recently, four structural features were identified for switching the H5 HA binding specificity from bird to human receptors and making H5N1 viruses more similar to human-transmissible viruses (11). A clade 2.2.1 sublineage virus has already acquired mutations for two of these features: deletion of the HA 130 loop of the RBD and loss of the 158 glycosylation sequence (10, 14, 24, 43) on the globular head. This indicates that mutations that change the primary structure of HA in the 130 loop, 220 loop, and 190 helix of the RBD may produce a sublineage virus with all the key features for switching host receptor specificity. We noted that the H5N1 variants from patients in Egypt in this study had changed their HA RBD primary structure, although this change may not have been sufficient for human adaptation because the human receptor binding specificity of these viruses was less than that of seasonal human viruses (Fig. 1). Therefore, H5N1 viruses in Egypt have a substantially higher pandemic potential than animal influenza viruses in other geographic areas.

The stability of HA has been proposed to be correlated with the environmental stability and airborne transmissibility of influenza viruses (17, 24, 44). In the ferret passage studies, additional mutations that stabilized HA were required for droplet transmission of H5N1 viruses among ferrets (17, 18). However, our data suggested that such mutations that stabilize HA have still not been detected in Egyptian patients and that the decrease in HA stability was a compensatory mechanism for the increase in viral replication in human airway epithelia, implying different mechanisms for H5N1 transmissibility and infectivity in humans. Herfst et al. (42) found that the majority of ferrets infected with the transmis-

sible H5N1 virus in their study survived. This suggested that H5N1 transmission in ferrets was accompanied by a loss of virulence (42, 44). However, the emergence of H5N1 variants with increased replicative efficiency may correlate with the severity of viral pathogenicity in infected individuals. Our data suggest that the emergence of variants with increased fitness for infecting the human airway environment might be a novel mechanism for increased pathogenicity in H5N1 infections. However, metagenomic analysis using archived RNA samples in the ferret transmission study (21) suggested that even minor variants with favorable HA mutations in infected individuals could be the source of airborne virus transmission (45). Our database search identified the major HA variants in viruses isolated from patients but did not consider minor variants that may have emerged. Future metagenomic approaches to quantify the variations in clinical virus isolates selected in H5N1-infected patients should provide an in-depth picture of the genetic diversity of human H5N1 viruses. Since this study was designed to investigate the fitness of H5N1 viruses in patients, the transmissibility of the variants identified in this study needs further careful study using ferret and/or guinea pig models under appropriate biosafety conditions.

In conclusion, our findings suggested that H5N1 viruses, at least clade 2.2.1 viruses, can rapidly adapt to the human respiratory tract microenvironment by mutations that alter the balance of HA properties in H5N1-infected patients. These data begin to clarify the picture of the mechanisms of H5N1 adaption for human infections.

## MATERIALS AND METHODS

**Ethics statement and biosecurity.** All studies using anonymized primary human cells were conducted under the applicable laws and approved by the Institutional Review Board of Osaka University (approval number 21-3). All animal studies were conducted under the applicable laws and guidelines for the care and use of laboratory animals and approved by the Animal Experiment Committee of the Research Institute for Microbial Diseases, Osaka University (approval number H24-07-1). All studies with recombinant DNAs were conducted under the applicable laws and approved by the Biological Safety Committee of the Research Institute for Microbial Diseases, Osaka University. All experiments with live H5N1 viruses were performed under biosafety level 3+ (BSL 3+) conditions at Osaka University (approval number 3439).

**Database search.** The published sequences of 437 HA genes from influenza A virus subtype H5N1 strains that were isolated in Egypt from 2006 to 2010 were obtained from the NCBI IVR (<http://www.ncbi.nlm.nih.gov/genomes/FLU/FLU.html>). These sequences were aligned by using the MAFFT program (46). HA mutations in the 94 human and 343 bird H5N1 virus strains were identified by comparing the HA sequences in these strains to a consensus HA sequence that was determined from the aligned sequences of all the Egyptian H5N1 HA sequences. The prevalences of the mutations in human and bird virus strains were then calculated and compared among the viruses isolated from the two hosts.

**Cells.** Chicken embryo fibroblasts (CEFs) were prepared from 10-day-old embryonated eggs. Human embryonic kidney 293T cells and Madin-Darby canine kidney (MDCK) cells were maintained in Dulbecco's modified Eagle's medium (DMEM) supplemented with 10% heat-inactivated fetal calf serum (FCS) at 37°C in a humidified atmosphere of 95% air and 5% CO<sub>2</sub> as previously described (47). Monkey kidney CV-1 cells were maintained in MEM supplemented with 5% heat-inactivated FCS. Primary SAE cells (Lonza Corporation) were maintained according to the manufacturer's recommendations.

**Virus preparation.** Avian and human influenza viruses were grown in 10-day-old embryonated chicken eggs and MDCK cells, respectively. The allantoic fluids and culture supernatants were then harvested and stored

as seed viruses at  $-80^{\circ}\text{C}$ . For subsequent studies, allantoic fluids and culture supernatants were purified by ultracentrifugation as described in Text S1 in the supplemental material. Viral titers were assayed as focus-forming units (FFU) by focus-forming assays (14) using MDCK cells.

**Generation of viruses by reverse genetics.** Recombinant viruses were generated with a plasmid-based reverse genetics system in the EG/D1 (wt) virus genetic background as previously described (14). Mutant HA genes were generated by PCR-based site-directed mutagenesis. All constructs were completely sequenced to ensure the absence of unwanted mutations. Recombinant viruses were propagated by single passage in eggs. The HA genes of the virus stocks were sequenced to detect the possible emergence of revertants during amplification.

**Hemagglutination assays.** Stocks of avian and human influenza viruses were serially diluted with phosphate-buffered saline (PBS) and mixed with 0.5% turkey red blood cells (Nippon Biotest) and 0.75% guinea pig red blood cells (Nippon Biotest), respectively. Hemagglutination by avian and human influenza viruses was observed after incubation at room temperature for 30 min and 1 h, respectively, to determine the titers of hemagglutinating units (HAU). To correct for differences in HAU because of different blood lots, a reference virus sample was used, and the HAU of each virus sample was calculated relative to the reference EG/D1 HAU titer.

**Receptor specificity assays.** Receptor binding specificity was analyzed by a solid-phase direct binding assay as described in Text S1 (Materials and Methods) in the supplemental material, using sialylglycopolymers with different numbers of LN (Gal $\beta$ 1,4GlcNAc) repeats (48).  $\alpha$ 2,3 SLN and  $\alpha$ 2,6 SLN denote Neu5Ac $\alpha$ 2-3 and Neu5Ac $\alpha$ 2-6, respectively, linked to LN.

**Viral growth kinetics in primary human cells.** Primary human airway epithelial cells were infected in triplicate with viruses at an MOI of 0.1. After 1 h at  $37^{\circ}\text{C}$ , the virus inoculum was removed, and the cells were washed with PBS, followed by further incubation at  $37^{\circ}\text{C}$ . Acetylated trypsin (0.5  $\mu\text{g}/\text{ml}$ ) was also added to the cell cultures for propagation of human viruses. At the times postinfection indicated in Fig. 2 and 3, viral titers in the cell culture supernatants were assayed by quantitative real-time RT-PCR and focus-forming assays.

**Quantitative real-time RT-PCR.** Progeny virus RNA was extracted from the culture medium of infected cells with a QIAamp viral RNA minikit (Qiagen) and assayed by quantitative real-time reverse transcription (RT)-PCR (QuantiTect probe RT-PCR kit, Qiagen), using primers targeting the M gene as previously described (49).

**Cell fusion assays.** CV-1 cells (90% confluent in 24-well plates) were transfected with HA expression plasmids using Lipofectamine LTX (Invitrogen) according to the manufacturer's recommendations. At 24 h posttransfection, the culture medium was replaced with PBS fusion buffer (PBS containing 1 mM  $\text{CaCl}_2$  and 0.5 mM  $\text{MgCl}_2$ ) at pH 5.2, 5.3, 5.4, 5.5, 5.6, 5.7, 5.8, 5.9, or 6.0 and incubated for 3 min. The cells were then washed once with PBS fusion buffer (pH 7.0) and returned to DMEM-F-12 (Invitrogen). After 3 h of incubation at  $37^{\circ}\text{C}$ , the cells were fixed with 4% buffered paraformaldehyde and stained with Giemsa stain solution. The pH threshold was the highest pH value at which polykaryon formation was observed.

**Thermostability.** Viruses (128 HAU in PBS) were incubated for the times indicated in Fig. S4 at  $50^{\circ}\text{C}$  or  $54^{\circ}\text{C}$ . Hemagglutination activity then was determined by hemagglutination assays. Thermostability data were plotted against the incubation time at  $50^{\circ}\text{C}$  or  $54^{\circ}\text{C}$  and analyzed using Origin 9.1 Data Analysis and Graphing Software (OriginLab). The data were fitted with the sigmoidal Boltzmann equation, and the decay times at which virus activity was reduced to 8 HAU were calculated.

**Experimental infection of mice.** To determine the 50% mouse lethal dose ( $\text{MLD}_{50}$ ), 5-week-old female BALB/c mice (Japan SLC), under isoflurane anesthesia, were inoculated intranasally with 75- $\mu\text{l}$  samples of serial 10-fold dilutions of virus in PBS. The mice were observed daily for 14 days for weight loss and mortality. From these data,  $\text{MLD}_{50}$  values were calculated by the Reed-Muench method and expressed as the FFU re-

quired for 1  $\text{MLD}_{50}$ . At 3 and 6 days after inoculation with  $3 \times 10^4$  FFU, virus titers in lungs were assayed as FFU in MDCK cells.

## SUPPLEMENTAL MATERIAL

Supplemental material for this article may be found at <http://mbio.asm.org/lookup/suppl/doi:10.1128/mBio.00081-15/-/DCSupplemental>.

Text S1, DOC file, 0.1 MB.  
Figure S1, PDF file, 0.7 MB.  
Figure S2, PDF file, 0.3 MB.  
Figure S3, PDF file, 0.1 MB.  
Figure S4, PDF file, 0.4 MB.  
Figure S5, PDF file, 0.1 MB.  
Figure S6, PDF file, 0.3 MB.  
Table S1, PDF file, 0.1 MB.  
Table S2, PDF file, 0.1 MB.  
Table S3, PDF file, 0.1 MB.

## ACKNOWLEDGMENTS

We thank K. Murata for the sequencing analyses and A. Yamashita for computational assistance and resources.

This work was supported by a Grant-in-Aid for Scientific Research from the Ministry of Education, Culture, Sports, Science and Technology of Japan (JSPS KAKENHI grants 23791134 and 23406017).

## REFERENCES

- García-Sastre A, Schmolke M. 2014. Avian influenza A H10N8—a virus on the verge? *Lancet* 383:676–677. [http://dx.doi.org/10.1016/S0140-6736\(14\)60163-X](http://dx.doi.org/10.1016/S0140-6736(14)60163-X).
- To KK, Tsang AK, Chan JF, Cheng VC, Chen H, Yuen KY. 2014. Emergence in China of human disease due to avian influenza A(H10N8)—cause for concern? *J Infect* 68:205–215. <http://dx.doi.org/10.1016/j.jinf.2013.12.014>.
- Peiris JS, de Jong MD, Guan Y. 2007. Avian influenza virus (H5N1): a threat to human health. *Clin Microbiol Rev* 20:243–267. <http://dx.doi.org/10.1128/CMR.00037-06>.
- Watanabe Y, Ibrahim MS, Suzuki Y, Ikuta K. 2012. The changing nature of avian influenza A virus (H5N1). *Trends Microbiol* 20:11–20. <http://dx.doi.org/10.1016/j.tim.2011.10.003>.
- Webster RG, Bean WJ, Gorman OT, Chambers TM, Kawaoka Y. 1992. Evolution and ecology of influenza A viruses. *Microbiol Rev* 56:152–179.
- Imai M, Kawaoka Y. 2012. The role of receptor binding specificity in interspecies transmission of influenza viruses. *Curr Opin Virol* 2:160–167. <http://dx.doi.org/10.1016/j.coviro.2012.03.003>.
- Skehel JJ, Wiley DC. 2000. Receptor binding and membrane fusion in virus entry: the influenza hemagglutinin. *Annu Rev Biochem* 69:531–569. <http://dx.doi.org/10.1146/annurev.biochem.69.1.531>.
- Brown JD, Goekjian G, Poulson R, Valeika S, Stallknecht DE. 2009. Avian influenza virus in water: infectivity is dependent on pH, salinity and temperature. *Vet Microbiol* 136:20–26. <http://dx.doi.org/10.1016/j.vetmic.2008.10.027>.
- Scholtissek C. 1985. Stability of infectious influenza A viruses at low pH and at elevated temperature. *Vaccine* 3:215–218. [http://dx.doi.org/10.1016/0264-410X\(85\)90109-4](http://dx.doi.org/10.1016/0264-410X(85)90109-4).
- Neumann G, Macken CA, Karasin AL, Fouchier RA, Kawaoka Y. 2012. Egyptian H5N1 influenza viruses—cause for concern? *PLoS Pathog* 8:e1002932. <http://dx.doi.org/10.1371/journal.ppat.1002932>.
- Tharakaraman K, Raman R, Viswanathan K, Stebbins NW, Jayaraman A, Krishnan A, Sasisekharan V, Sasisekharan R. 2013. Structural determinants for naturally evolving H5N1 hemagglutinin to switch its receptor specificity. *Cell* 153:1475–1485. <http://dx.doi.org/10.1016/j.cell.2013.05.035>.
- Watanabe Y, Ibrahim MS, Ikuta K. 2013. Evolution and control of H5N1. A better understanding of the evolution and diversity of H5N1 flu virus and its host species in endemic areas could inform more efficient vaccination and control strategies. *EMBO Rep* 14:117–122. <http://dx.doi.org/10.1038/embor.2012.212>.
- Perovic VR, Muller CP, Niman HL, Veljkovic N, Dietrich U, Tosic DD, Glisic S, Veljkovic V. 2013. Novel phylogenetic algorithm to monitor human tropism in Egyptian H5N1-HPAIV reveals evolution toward effi-

- cient human-to-human transmission. *PLoS One* 8:e61572. <http://dx.doi.org/10.1371/journal.pone.0061572>.
14. Watanabe Y, Ibrahim MS, Ellakany HF, Kawashita N, Mizuike R, Hiramatsu H, Sriwilajaroen N, Takagi T, Suzuki Y, Ikuta K. 2011. Acquisition of human-type receptor binding specificity by new H5N1 influenza virus sublineages during their emergence in birds in Egypt. *PLoS Pathog* 7:e1002068. <http://dx.doi.org/10.1371/journal.ppat.1002068>.
  15. Chandrasekaran A, Srinivasan A, Raman R, Viswanathan K, Raguram S, Tumpey TM, Sasisekharan V, Sasisekharan R. 2008. Glycan topology determines human adaptation of avian H5N1 virus hemagglutinin. *Nat Biotechnol* 26:107–113. <http://dx.doi.org/10.1038/nbt1375>.
  16. Matrosovich M, Tuzikov A, Bovin N, Gambaryan A, Klimov A, Castrucci MR, Donatelli I, Kawaoka Y. 2000. Early alterations of the receptor-binding properties of H1, H2 and H3 avian influenza virus hemagglutinins after their introduction into mammals. *J Virol* 74:8502–8512.
  17. Imai M, Herfst S, Sorrell EM, Schrauwen EJ, Linster M, De Graaf M, Fouchier RA, Kawaoka Y. 2013. Transmission of influenza A/H5N1 viruses in mammals. *Virus Res* 178:15–20. <http://dx.doi.org/10.1016/j.virusres.2013.07.017>.
  18. Linster M, van Boheemen S, de Graaf M, Schrauwen EJ, Lexmond P, Mänz B, Bestebroer TM, Baumann J, van Riel D, Rimmelzwaan GF, Osterhaus AD, Matrosovich M, Fouchier RA, Herfst S. 2014. Identification, characterization, and natural selection of mutations driving airborne transmission of A/H5N1 virus. *Cell* 157:329–339. <http://dx.doi.org/10.1016/j.cell.2014.02.040>.
  19. Carr CM, Chaudhry C, Kim PS. 1997. Influenza hemagglutinin is spring-loaded by a metastable native conformation. *Proc Natl Acad Sci U S A* 94:14306–14313. <http://dx.doi.org/10.1073/pnas.94.26.14306>.
  20. Haywood AM, Boyer BP. 1986. Time and temperature dependence of influenza virus membrane fusion at neutral pH. *J Gen Virol* 67(Pt 12): 2813–2817. <http://dx.doi.org/10.1099/0022-1317-67-12-2813>.
  21. Imai M, Watanabe T, Hatta M, Das SC, Ozawa M, Shinya K, Zhong G, Hanson A, Katsura H, Watanabe S, Li C, Kawakami E, Yamada S, Kiso M, Suzuki Y, Maher EA, Neumann G, Kawaoka Y. 2012. Experimental adaptation of an influenza H5 HA confers respiratory droplet transmission to a reassortant H5 HA/H1N1 virus in ferrets. *Nature* 486:420–428. <http://dx.doi.org/10.1038/nature10831>.
  22. Yong E. 2012. Mutant-flu paper published. *Nature* 485:13–14. <http://dx.doi.org/10.1038/485013a>.
  23. Palese P, Wang TT. 2012. H5N1 influenza viruses: facts, not fear. *Proc Natl Acad Sci U S A* 109:2211–2213. <http://dx.doi.org/10.1073/pnas.1121297109>.
  24. De Graaf M, Fouchier RA. 2014. Role of receptor binding specificity in influenza A virus transmission and pathogenesis. *EMBO J* 33:823–841. <http://dx.doi.org/10.1002/embj.201387442>.
  25. Auewarakul P, Suptawitwan O, Kongchanagul A, Sangma C, Suzuki Y, Ungchusak K, Louisirotranachakul S, Lerdsamran H, Pooruk P, Thitithanyanont A, Pittayawonganon C, Guo CT, Hiramatsu H, Jampangern W, Chunsutthiwat S, Puthavathana P. 2007. An avian influenza H5N1 virus that binds to a human-type receptor. *J Virol* 81:9950–9955. <http://dx.doi.org/10.1128/JVI.00468-07>.
  26. Walther T, Karamanska R, Chan RW, Chan MC, Jia N, Air G, Hopton C, Wong MP, Dell A, Malik Peiris JS, Haslam SM, Nicholls JM. 2013. Glycomic analysis of human respiratory tract tissues and correlation with influenza virus infection. *PLoS Pathog* 9. <http://dx.doi.org/10.1371/journal.ppat.1003223>.
  27. Lakadamyali M, Rust MJ, Zhuang X. 2004. Endocytosis of influenza viruses. *Microbes Infect* 6:929–936. <http://dx.doi.org/10.1016/j.micinf.2004.05.002>.
  28. Murakami S, Horimoto T, Ito M, Takano R, Katsura H, Shimojima M, Kawaoka Y. 2012. Enhanced growth of influenza vaccine seed viruses in Vero cells mediated by broadening the optimal pH range for virus membrane fusion. *J Virol* 86:1405–1410. <http://dx.doi.org/10.1128/JVI.06009-11>.
  29. DuBois RM, Zaraket H, Reddivari M, Heath RJ, White SW, Russell CJ. 2011. Acid stability of the hemagglutinin protein regulates H5N1 influenza virus pathogenicity. *PLoS Pathog* 7:e1002398. <http://dx.doi.org/10.1371/journal.ppat.1002398>.
  30. Galloway SE, Reed ML, Russell CJ, Steinhauer DA. 2013. Influenza HA subtypes demonstrate divergent phenotypes for cleavage activation and pH of fusion: implications for host range and adaptation. *PLoS Pathog* 9:e1003151. <http://dx.doi.org/10.1371/journal.ppat.1003151>.
  31. Washington N, Steele RJ, Jackson SJ, Bush D, Mason J, Gill DA, Pitt K, Rawlins DA. 2000. Determination of baseline human nasal pH and the effect of intranasally administered buffers. *Int J Pharm* 198:139–146. [http://dx.doi.org/10.1016/S0378-5173\(99\)00442-1](http://dx.doi.org/10.1016/S0378-5173(99)00442-1).
  32. Brown EG, Liu H, Kit LC, Baird S, Nesrallah M. 2001. Pattern of mutation in the genome of influenza A virus on adaptation to increased virulence in the mouse lung: identification of functional themes. *Proc Natl Acad Sci U S A* 98:6883–6888. <http://dx.doi.org/10.1073/pnas.111165798>.
  33. Keleta L, Ibricevic A, Bovin NV, Brody SL, Brown EG. 2008. Experimental evolution of human influenza virus H3 hemagglutinin in the mouse lung identifies adaptive regions in HA1 and HA2. *J Virol* 82: 11599–11608. <http://dx.doi.org/10.1128/JVI.01393-08>.
  34. Ping J, Keleta L, Forbes NE, Dankar S, Stecho W, Tyler S, Zhou Y, Babiuk L, Weingartl H, Halpin RA, Boyne A, Bera J, Hostetler J, Fedorova NB, Proudfoot K, Katzel DA, Stockwell TB, Ghedin E, Spiro DJ, Brown EG. 2011. Genomic and protein structural maps of adaptive evolution of human influenza A virus to increased virulence in the mouse. *PLoS One* 6:e21740. <http://dx.doi.org/10.1371/journal.pone.0021740>.
  35. Krenn BM, Egorov A, Romanovskaya-Romanko E, Wolschek M, Nakowitsch S, Ruthsatz T, Kiefmann B, Morokutti A, Humer J, Geiler J, Cinatl J, Michaelis M, Wressnigg N, Sturlan S, Ferko B, Batishchev OV, Indenbom AV, Zhu R, Kastner M, Hinterdorfer P, Kiselev O, Muster T, Romanova J. 2011. Single HA2 mutation increases the infectivity and immunogenicity of a live attenuated H5N1 intranasal influenza vaccine candidate lacking NS1. *PLoS One* 6:e18577. <http://dx.doi.org/10.1371/journal.pone.0018577>.
  36. Cotter CR, Jin H, Chen Z. 2014. A single amino acid in the stalk region of the H1N1pdm influenza virus HA protein affects viral fusion, stability and infectivity. *PLoS Pathog* 10:e1003831. <http://dx.doi.org/10.1371/journal.ppat.1003831>.
  37. Zaraket H, Bridges OA, Duan S, Baranovich T, Yoon SW, Reed ML, Salomon R, Webby RJ, Webster RG, Russell CJ. 2013. Increased acid stability of the hemagglutinin protein enhances H5N1 influenza virus growth in the upper respiratory tract but is insufficient for transmission in ferrets. *J Virol* 87:9911–9922. <http://dx.doi.org/10.1128/JVI.01175-13>.
  38. Chen LM, Blixt O, Stevens J, Lipatov AS, Davis CT, Collins BE, Cox NJ, Paulson JC, Donis RO. 2012. In vitro evolution of H5N1 avian influenza virus toward human-type receptor specificity. *Virology* 422:105–113. <http://dx.doi.org/10.1016/j.virol.2011.10.006>.
  39. Chutinimitkul S, van Riel D, Munster VJ, van den Brand JM, Rimmelzwaan GF, Kuiken T, Osterhaus AD, Fouchier RA, de Wit E. 2010. In vitro assessment of attachment pattern and replication efficiency of H5N1 influenza A viruses with altered receptor specificity. *J Virol* 84:6825–6833. <http://dx.doi.org/10.1128/JVI.02737-09>.
  40. Crusat M, Liu J, Palma AS, Childs RA, Liu Y, Wharton SA, Lin YP, Coombs PJ, Martin SR, Matrosovich M, Chen Z, Stevens DJ, Hien VM, Thanh TT, Nhu le NT, Nguyet LA, Ha do Q, van Doorn HR, Hien TT, Conradt HS, Kiso M, Gamblin SJ, Chai W, Skehel JJ, Hay AJ, Farrar J, de Jong MD, Feizi T. 2013. Changes in the hemagglutinin of H5N1 viruses during human infection—influence on receptor binding. *Virology* 447:326–337. <http://dx.doi.org/10.1016/j.virol.2013.08.010>.
  41. Yamada S, Suzuki Y, Suzuki T, Le MQ, Nidom CA, Sakai-Tagawa Y, Muramoto Y, Ito M, Kiso M, Horimoto T, Shinya K, Sawada T, Kiso M, Usui T, Murata T, Lin Y, Hay A, Haire LF, Stevens DJ, Russell RJ, Gamblin SJ, Skehel JJ, Kawaoka Y. 2006. Haemagglutinin mutations responsible for the binding of H5N1 influenza A viruses to human-type receptors. *Nature* 444:378–382. <http://dx.doi.org/10.1038/nature05264>.
  42. Herfst S, Schrauwen EJ, Linster M, Chutinimitkul S, de Wit E, Munster VJ, Sorrell EM, Bestebroer TM, Burke DF, Smith DJ, Rimmelzwaan GF, Osterhaus AD, Fouchier RA. 2012. Airborne transmission of influenza A/H5N1 virus between ferrets. *Science* 336:1534–1541. <http://dx.doi.org/10.1126/science.1213362>.
  43. Watanabe Y, Ibrahim MS, Ellakany HF, Kawashita N, Daidoji T, Takagi T, Yasunaga T, Nakaya T, Ikuta K. 2012. Antigenic analysis of highly pathogenic avian influenza virus H5N1 sublineages co-circulating in Egypt. *J Gen Virol* 93:2215–2226. <http://dx.doi.org/10.1099/vir.0.044032-0>.
  44. Miller MS, Palese P. 2014. Peering into the crystal ball: influenza pandemics and vaccine efficacy. *Cell* 157:294–299. <http://dx.doi.org/10.1016/j.cell.2014.03.023>.
  45. Wilker PR, Dinis JM, Starrett G, Imai M, Hatta M, Nelson CW, O'Connor DH, Hughes AL, Neumann G, Kawaoka Y, Friedrich TC. 2013. Selection on haemagglutinin imposes a bottleneck during mamma-

- lian transmission of reassortant H5N1 influenza viruses. *Nat Commun* 4:2636.
46. Katoh K, Misawa K, Kuma K, Miyata T. 2002. MAFFT: a novel method for rapid multiple sequence alignment based on fast Fourier transform. *Nucleic Acids Res* 30:3059–3066. <http://dx.doi.org/10.1093/nar/gkf436>.
  47. Watanabe Y, Ohtaki N, Hayashi Y, Ikuta K, Tomonaga K. 2009. Autogenous translational regulation of the Borna disease virus negative control factor X from polycistronic mRNA using host RNA helicases. *PLoS Pathog* 5:e1000654. <http://dx.doi.org/10.1371/journal.ppat.1000654>.
  48. Hidari KI, Murata T, Yoshida K, Takahashi Y, Minamijima YH, Miwa Y, Adachi S, Ogata M, Usui T, Suzuki Y, Suzuki T. 2008. Chemoenzymatic synthesis, characterization, and application of glycopolymers carrying lactosamine repeats as entry inhibitors against influenza virus infection. *Glycobiology* 18:779–788. <http://dx.doi.org/10.1093/glycob/cwn067>.
  49. Watanabe Y, Ibrahim MS, Ellakany HF, Abd El-Hamid HS, Ikuta K. 2011. Genetic diversification of H5N1 highly pathogenic avian influenza A virus during replication in wild ducks. *J Gen Virol* 92:2105–2110. <http://dx.doi.org/10.1099/vir.0.032623-0>.